Dalton Transactions

PAPER

View Article Online
View Journal | View Issue

Cite this: *Dalton Trans.*, 2016, **45**, 6383

An investigation of the interactions of Eu^{3+} and Am^{3+} with uranyl minerals: implications for the storage of spent nuclear fuel†

Saptarshi Biswas,[a] Robin Steudtner,[b] Moritz Schmidt,[b] Cora McKenna,[c] Luis León Vintró,[d] Brendan Twamley[a] and Robert J. Baker*[a]

Received 15th January 2016,
Accepted 29th February 2016

DOI: 10.1039/c6dt00199h

www.rsc.org/dalton

The reaction of a number of uranyl minerals of the (oxy)hydroxide, phosphate and carbonate types with Eu(III), as a surrogate for Am(III), have been investigated. A photoluminescence study shows that Eu(III) can interact with the uranyl minerals $Ca[(UO_2)_6(O)_4(OH)_6]\cdot 8H_2O$ (becquerelite) and $A[UO_2(CO_3)_3]\cdot xH_2O$ (A/x = $K_3Na/1$, grimselite; $CaNa_2/6$, andersonite; and $Ca_2/11$, liebigite). For the minerals $[(UO_2)_8(O)_2(OH)_{12}]\cdot 12H_2O$ (schoepite), $K_2[(UO_2)_6(O)_4(OH)_6]\cdot 7H_2O$ (compreignacite), $A[(UO_2)_2(PO_4)_2]\cdot 8H_2O$ (A = Ca, *meta*-autunite; Cu, *meta*-torbernite) and $Cu[(UO_2)_2(SiO_3OH)_2]\cdot 6H_2O$ (cuprosklodowskite) no Eu(III) emission was observed, indicating no incorporation into, or sorption onto the structure. In the examples with Eu^{3+} incorporation, sensitized emission is seen and the lifetimes, hydration numbers and quantum yields have been determined. Time Resolved Laser Induced Fluroescence Spectroscpoy (TRLFS) at 10 K have also been measured and the resolution enhancements at these temperatures allow further information to be derived on the sites of Eu(III) incorporation. Infrared and Raman spectra are recorded, and SEM analysis show significant morphology changes and the substitution of particularly Ca^{2+} by Eu^{3+} ions. Therefore, Eu^{3+} can substitute Ca^{2+} in the interlayers of becquerelite and liebigite and in the structure of andersonite, whilst in grimselite only sodium is exchanged. These results have guided an investigation into the reactions with ^{241}Am on a tracer scale and results from gamma-spectrometry show that becquerelite, andersonite, grimselite, liebigite and compreignacite can include americium in the structure. Shifts in the U=O and C–O Raman active bands are similar to that observed in the Eu(III) analogues and Am(III) photoluminescence measurements are also reported on these phases; the Am^{3+} ion quenches the emission from the uranyl ion.

Introduction

The safe storage of legacy, current and future spent nuclear fuels (SNF) is one of society's grand challenges. Current EU policy is to store the highly radioactive materials over long timescales (10^6 years) in suitable underground repositories.[1] A geological repository can possibly have both an oxidising and reducing environment.[2] Under reducing conditions uraninite (UO_{2+x}) or coffinite ($USiO_4$) are the dominant minerals that would be formed, but a study of the chemistry of coffinite has been hampered by the difficulty in synthesising pure material.[3] Under oxidizing conditions, UO_2 (the major component of SNF) is thermodynamically unstable and will oxidise to UO_3 *via* a number of phase transitions, some of which have been experimentally characterised.[4] Interestingly, these phases interact with other radionuclides *via* a number of mechanisms and can inhibit or accelerate the mobility of these species. The most studied radioisotope in this regard is neptunium as Np(V) is very soluble in groundwater with low adsorption onto the geomatrix[5] which, combined with a high radiotoxicity, makes it especially important to understand the underlying chemistry. The mechanism of incorporation is still uncertain, but a charge balancing substitution of $[NpO_2]^+$ and M^+ for $[UO_2]^{2+}$ has been postulated for a number of minerals[6] whilst co-precipitation of a distinct Np_2O_5 phase[7] or direct substitution[8] of $[UO_2]^{2+}$ for $[NpO_2]^{2+}$ has also been observed.

Based on an analysis of the crystal chemistry of uranyl minerals, it was predicted that the substitution of An(III) (An = Pu, Am, Cm) may occur either at the interlayer sites or in the

[a]*School of Chemistry, University of Dublin, Trinity College, Dublin 2, Ireland. E-mail: bakerrj@tcd.ie*
[b]*Helmholtz-Zentrum Dresden-Rossendorf e.V., Institute of Resource Ecology, P.O. Box 510119, D-01314 Dresden, Germany*
[c]*Department of Geology, School of Natural Sciences, University of Dublin, Trinity College, Dublin 2, Ireland*
[d]*School Of Physics, University College Dublin, Belfield, Dublin 4, Ireland*
†Electronic supplementary information (ESI) available: Further spectroscopic and structural data. See DOI: 10.1039/c6dt00199h

sheets of minerals,[9] as has been observed with Np. Whilst americium is not a major principle component of SNF (*ca.* 0.06 wt%), decay of ^{241}Pu, which is a significant fraction of irradiated fuel, means that ^{241}Am is a grow-in product. Current calculations suggest 594 g Am (as 503 g ^{241}Am, 0.66 g ^{242m}Am and 90.6 g ^{243}Am, or 64.5 TBq of radiation) per metric ton of uranium will be present after 10 year decay.[10] Therefore, the build-up of Am becomes extremely significant for the later timeframe. Comparatively little research has been published upon how americium behaves under environmental conditions, likely due to the high specific activity of this isotope, but it is known that the +3 oxidation state dominates for Am under environmental conditions.[11] Whilst Am(III) sorption and incorporation studies have been reported using minerals such as calcite ($CaCO_3$), aluminium or iron oxides and hydroxides or clay materials,[12] studies with uranyl minerals are almost non-existent. We recently reported that studtite, $[UO_2(\eta^2\text{-}O_2)(H_2O)_2]\cdot 2H_2O$, does not incorporate ^{241}Am(III) on tracer scales,[13] in keeping with earlier investigations of *meta*-studtite on the surface of SNF.[14] Due to the radiological issues surrounding the use of Am, the lanthanide europium has commonly been used as a surrogate, given that these 4f and 5f ions generally display similar chemistry and the eight coordinate ionic radii are comparable (Eu(III) = 107 pm; Am(III) = 109 pm).[15] Moreover, the photophysical properties of Eu(III) lend itself to a very useful spectroscopic probe for both site-symmetry determination and hydration numbers.[16] For example, the interaction of Eu(III) ions with the surface of α-uranophane showed that the europium ion does bind to the surface *via* the formation of an inner-sphere complex over a broad pH range.[17] Eu(III) and Nd(III) have been shown to insert into the interlayer spaces of a synthetic uranyl vanadate whereby the Eu ion is linked throughout the structure by V=O–Eu cation–cation interactions, and uranyl sensitization of lanthanide emission was not observed.[18] The use of Ce(IV) and Nd(III) as surrogates for Pu(IV) and Am(III) has shown that a significant amount of these ions can be incorporated into both ianthinite ($[U^{IV}(UO_2)_5O_7]\cdot 10H_2O$) and becquerelite ($Ca[(UO_2)_6(O)_4(OH)_6]\cdot 8H_2O$), *via* a charge coupled substitution of $Nd^{3+} + O^{2-}$ with $Ca^{2+} + OH^-$; no emission data were described.[19] In this report we show that Eu(III) can interact with selected uranyl containing minerals, and have characterized the mechanism *via* the use of emission spectroscopy. For some examples sensitized europium emission is observed (*i.e.* excitation at a wavelength typical for uranyl ion is followed by energy transfer to a Eu(III) excited state and subsequent emission to the Eu(III) ground state), which gives a valuable insight into the structures of these complexes. Furthermore, emission spectroscopy conducted at 10 K also sheds light onto the environment around the europium and hence gives further structural information. The phases have also been characterized by ICP-MS, vibrational spectroscopy and scanning electron microscopy with energy dispersive X-ray spectroscopy (SEM-EDX). The europium experiments have guided us towards minerals that might sorb americium and we have studied these interactions on a tracer scale. Gamma-spectrometry has allowed us to quantify the extent of ^{241}Am sorption and vibrational and photoluminescence spectroscopy is also presented.

Results and discussion

We have synthesized and characterized nine uranyl mineral phases for this work. The photophysical properties of the minerals chosen have been reported previously, and the uranyl emission spectra in our hands are included in the ESI (Fig. S1†). Grimselite has not been previously characterized by emission spectroscopy and the emission and excitation spectra are shown in Fig. S2,† which is typical for a uranyl compound. The emission spectra of other $A_4[UO_2(CO_3)_3]$ that feature group 1 or 2 cations, such as andersonite (A = Na_2Ca),[20] swartzite (A = MgCa)[21] or liebigite (A = Ca_2)[22] are essentially identical, as might be expected based upon the similarity in structure. The room temperature uranyl emission lifetime for grimselite is 80 ± 8 μs, although it should be noted that this is of secondary concern in uranyl minerals; for comparison andersonite has a reported uranyl emission lifetime of 65 ± 0.6 μs, swartzite 59.4 ± 0.1 μs and liebigite the longest at 313 μs at room temperature.

Europium(III) complexes

In order to model the chemistry of americium, we have approached the photochemistry aspect of this work in two ways: the reaction of prepared uranyl minerals with Eu(III) (a contacting process) and by the synthesis of the minerals in the presence of Eu(III) (a co-precipitation methodology).

Uranyl phosphates and silicates. Uranyl phosphate and silicate minerals are formed under phosphate or silicate rich environmental conditions and thus an important and widespread source of insoluble uranium compounds in soils. *meta*-Autunite ($Ca[(UO_2)_2(PO_4)_2]\cdot 8H_2O$), *meta*-torbernite ($Cu[(UO_2)_2(PO_4)_2]\cdot 8H_2O$) and cuprosklodowskite ($Cu[(UO_2)_2(SiO_3OH)_2]\cdot 6H_2O$) show no change in the emission or vibrational spectra under both experimental conditions, so we conclude that Eu(III) does not sorb onto the surface or exchange with the cations.

Uranyl (oxy)hydroxides. These compounds are known to form during the initial oxidation[4] of UO_2 so we explored the reactions of Eu(III) with schoepite, $[(UO_2)_8O_2(OH)_{12}]\cdot 12H_2O$, compreignacite, $K_2[(UO_2)_6O_4(OH)_6]\cdot 7H_2O$ and becquerelite, $Ca[(UO_2)_6(O)_4(OH)_6]\cdot 8H_2O$, under both experimental conditions. The structures of these species consist of layers of uranyl (oxy) hydroxides with water (schoepite), potassium (compreignacite) or calcium (becquerelite, Fig. S3†) in the interlayers, and these cations interact with the –yl oxygen, generally termed cation–cation interactions (CCIs). No evidence of Eu(III) incorporation into the minerals *via* the contacting process was observed, whilst co-precipitation of schoepite or compreignacite with Eu(III) also afforded no Eu(III) incorporation. In contrast, the powder isolated from the synthesis of becquerelite in the presence of Eu(III) showed only europium emission (Fig. 1a and S4† displays the uranyl region), even when excited at wave-

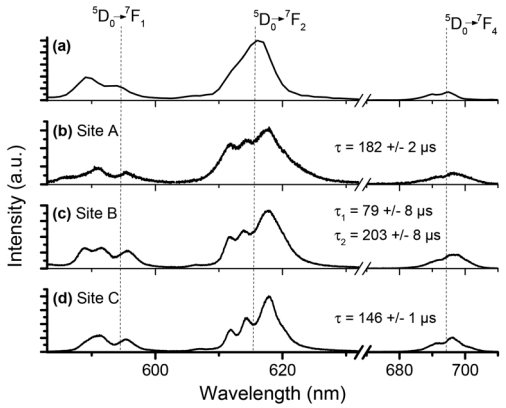

Fig. 1 Solid-state emission spectra of Eu(III) incorporated in becquerelite. (a) λ_{ex} = 350 nm; T = 300 K; (b) λ_{ex} = 578.08 nm; T = 10 K; (c) λ_{ex} = 579.18 nm; T = 10 K; (d) λ_{ex} = 579.53 nm; T = 10 K.

Table 1 Vibrational data for becquerelite and the corresponding Eu(III) complexes including the Eu(III) lifetime data

Mineral	ν_1(U=O) cm^{-1}	ν_3(U=O) cm^{-1}	τ(RT) μs	τ(10 K) μs
Becquerelite	796 829	872 908	—	—
D-Becquerelite	821	948 872 806	—	—
Becquerelite + Eu	796 822	910	26, 63	A: 182 ± 2 B: 203 ± 8; 79 ± 28 C: 146 ± 1
D-Becquerelite + Eu	826	906 870 824	26, 106	

lengths (λ_{ex} = 350 or 450 nm) that was specific to uranyl, *i.e.* sensitized emission, which has previously been observed in a number of uranyl compounds.[23] In addition the excitation spectra show the presence of the U=O charge transfer band at *ca.* 430 nm (Fig. S5†). This suggests close proximity of the two ions to enable energy transfer to occur.

There are a number of features that are noteworthy: the $^5D_0 \rightarrow {}^7F_0$ transition (λ_{em} = 579 nm) is not observed and the ratio $I(^5D_0 \rightarrow {}^7F_2)/I(^5D_0 \rightarrow {}^7F_1)$ = 2.70 which suggests low symmetry of the Eu ions. The lifetime of the emission at room temperature (Table 1) shows a multi-exponential decay with a short and long component to the lifetime, possibly indicating more than one Eu(III) species is present. Finally the quantum yield has been measured (Φ = 0.2%) and is much lower compared to $EuCl_3$ (in our hands Φ = 1.35%), suggesting energy transfer is not efficient.

In order to calculate the hydration number using the established relationship to the lifetimes of the water and D_2O coordinated Eu(III) compounds *viz.* $q = 1.05[1/\tau_{H_2O} - 1/\tau_{D_2O}]$,[24] we also prepared the deuterated analogue by synthesis of becquerelite in D_2O followed by the addition of $EuCl_3$ in D_2O. The vibrational data of deuterated becquerelite shows small differences (Fig. S6 and S7†).[25] The lifetime of this compound in H_2O shows a short and long component. The short lifetime is shorter than for a fully hydrated Eu^{3+} ion, and this may point to a non-radiative de-excitation mechanism *via* the uranyl ion; similar effects on the Eu(III) lifetimes have been observed with transition metals, for example iron[26] or molybdate ions.[27] Alternatively, CCI's have been implicated in the short (500 μs) lifetime of the structural characterized $K_4[(UO_2)Eu_2(Ge_2O_7)_2]$.[23a] However, from the longer europium lifetimes of these compounds with H_2O and D_2O coordinated to the Eu(III) we were able to determine q = 6.4 ± 0.5. This suggests that the Eu(III) has lost two water molecules from its hydration sphere, as was previously observed in α-uranophane.[17] By considering the structure of becquerelite (Fig. S3†), this could happen either on the mineral surface, or by Ca^{2+} substitution in the cation inter-layer that link the layers of uranyl (oxy) hydroxides.

To further investigate this mechanism, SEM-EDX measurements were conducted. SEM images (Fig. S8†) show a large morphology change upon addition of Eu(III), and EDX (Fig. S9†) showed no calcium in the product. As EDX is semi-quantitative, we have also used ICP-MS techniques to quantify the U/Eu ratio of the phase digested in nitric acid, which for becquerelite is 12.0. Therefore, the spectroscopic data strongly suggest that Eu^{3+} can replace calcium ions in the interlayer spaces of the uranyl (oxy)hydroxide. Given the small differences in ionic radii (Eu^{3+} = 109 pm; Ca^{2+} = 114 pm with a six fold coordination number)[15] this is not unexpected, and has been observed in other Ca containing minerals such as calcite.[28] Moreover, from the U : Eu ratio we can suggest that the reaction that occurs (eqn (1)) is the same as the Nd reactivity previously postulated,[19] although the replacement of $2Eu^{3+}$ for $3Ca^{2+}$ may also be possible.

$$2Ca\left[(UO_2)_6O_4(OH)_6\right]\cdot 8H_2O + H^+ + Eu_{(aq)}{}^{3+} \rightarrow Eu\left[(UO_2)_{12}O_7(OH)_{13}\right]\cdot 8H_2O + 2Ca_{(aq)}{}^{2+} \quad (1)$$

As the room temperature emission spectra of Eu(III) incorporated becquerelite was very broad and, as such, gives little structural information, we next investigated the emission spectrum at 10 K. Careful examination of the excitation spectrum (Fig. S10†) showed three distinct Eu(III) species present (λ_{ex} = 578.08 nm; 579.18 nm; 579.53 nm) and their respective site selective emission spectra are shown in Fig. 1(b)–(d). There is an increase in the resolution of the spectra upon lowering the temperature which allows us to comment upon the symmetry of each emitting species, bearing in mind that the bands are still rather broad. The lifetimes of each were also measured and are shown in Fig. 1. There are two species, sites A and B which show the same emission profile, and this suggests a D_2 site symmetry, whilst site C has S_4 site symmetry.[16,29] Using the equation,[24,30] $q = 1.07(1/\tau_{H_2O}) - 0.62$, the hydration numbers are for site A = 5.3 ± 0.5, site B = 12.9 ± 0.5 and 4.6 ± 0.5 and site C = 6.7 ± 0.5; data for sites A and C suggest an

inner-sphere complexation of Eu(III) in the mineral. The short lifetime for site B could again be ascribed to the sensitized emission.

To corroborate the emission studies, the infrared and Raman spectra were measured (Table 1 and Fig. S6, S7†). These spectra show a slight shift to lower wavenumbers of the U=O stretch. An empirical relationship between the stretching frequency (cm^{-1}) and the bond length (r in pm) in uranyl minerals was first reported by Bartlett and Cooney:[31] $r = 10650[\nu_1(U{=}O)]^{-2/3} + 57.5$ and $r = 9141[\nu_3(U{=}O]^{-2/3} + 80.4$, shows that upon Eu^{3+} incorporation the U=O bond length doesn't change. There may be two important factors influencing the U=O bond length, namely cation–cation interactions and ligand-to-metal σ- and π-donation from the equatorial ligands.[32] Given the vibrational data does not support a significant change in the equatorial ligand coordination, a change from Ca^{2+} to Eu^{3+} in the cation–cation interaction may be expected to produce the only effect. The slight shifts in the U=O stretch infers that the Eu(III) interacts with uranyl oxygens. As the SEM images suggest a large change in morphology upon addition of Eu(III) and the substitution of Ca^{2+} for Eu^{3+} in the interlayer cations a disruption to the hydrogen bonding network would likely result; there are 8 symmetry distinct water molecules in the interlayers calcium ions from a structural analysis[33] but only 5–7 coordinated to Eu(III). Using the known empirical formula for converting the O–H stretching frequency to an O···O bonding distance,[34] we calculate 2.632 Å (2906 cm^{-1}), 2.741 Å (3291 cm^{-1}), 2.820 Å (3426 cm^{-1}) and 3.205 Å (3583 cm^{-1}) in europium incorporated becquerelite, compared to 2.708, 2.721 and 2.989 Å in becquerelite, although the broadness of the infrared bands does suggest these values should be used with caution.[35] Therefore, the spectroscopic data suggests that europium substitutes calcium in the interlayers and the europium coordination sphere consists of water molecules and cation–cation interactions to uranyl –yl oxygens that link two sheets of uranyl polyhedra together.

Uranyl carbonates. Given the fact that carbonate rocks and cement-based components will be omnipresent in any nuclear waste storage facility, we also examined three uranyl carbonate minerals namely andersonite, grimselite and liebigite. These compounds have different solid-state structures, so this influence can be explored. Liebigite has a layer structure (Fig. S11†), somewhat similar to becquerelite with hydrated calcium ion in the interlayer spaces and no interactions with the uranyl oxygen.[36] Andersonite[37] (Fig. S12†) and grimselite[38] (Fig. S13†) have a three dimensional structure, reminiscent of zeolites, with voids in the structures filled with water molecules; however in grimselite all the group 1 metal ions interact with the –yl oxygen *via* cation–cation interactions, but in andersonite CCIs are absent. It is worth noting that Eu^{3+} incorporation into calcite ($CaCO_3$) has been well studied by TRLFS methodologies.[28]

When andersonite is contacted with Eu(III) the resulting powder shows an emission spectrum that contains both uranyl and europium emission (Fig. 2). If the powders are washed

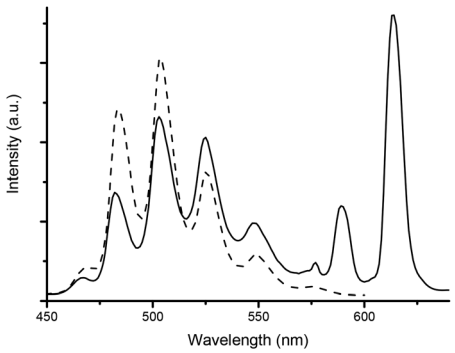

Fig. 2 Solid-state emission spectra of andersonite contacted with Eu(III) (λ_{ex} = 380 nm; solid line) and treated with aqueous EDTA (dashed line).

with a 0.1 M aqueous EDTA solution the europium emission is no longer present. The lifetime of the Eu^{3+} emission (212 ± 5 μs) suggests a water coordination number $q = 4.4 \pm 0.5$. The Raman spectra show no changes in the U=O and C–O bands when Eu(III) is added. These results are consistent with a weak inner sphere sorption of Eu(III) onto the surface.

Using the co-precipitation methodology of mixing uranyl nitrate, calcium nitrate, sodium carbonate and europium(III) chloride in water, a yellow powder precipitated over the course of 2 weeks. The room temperature emission spectrum of this powder is shown in Fig. S4.† In contrast to the contacting process only europium emission is observed, irrespective of the excitation wavelength *i.e.* sensitized emission. As in Becquerelite, the absence of a $^5D_0 \rightarrow {}^7F_0$ transition and the $I(^5D_0 \rightarrow {}^7F_2)/I(^5D_0 \rightarrow {}^7F_1)$ ratio of 2.44 suggest a low symmetry environment. At room temperature, splitting of the $^5D_0 \rightarrow {}^7F_{1,2}$ transitions are evident, whilst at low temperatures (Fig. 3) the $^5D_0 \rightarrow {}^7F_1$ transition resolves into three peak; this is consistent with D_2 site symmetry. Moreover only one Eu(III) species is present according to the excitation spectrum (Fig. S10†). The lifetime of the emission at room temperature shows a short and long component, with the longer giving a hydration number of 2.8 ± 0.5. The quantum yield (Φ = 0.73%) is again lower than $EuCl_3$. At low temperatures a single exponential decay is observed (τ = 580 ± 8 μs) corresponding to $q = 1.2 \pm 0.5$. SEM (Fig. S14†) images again show a morphology change upon addition of Eu(III), and EDX (Fig. S15†) analysis shows that no sodium or calcium is present – *i.e.* Eu^{3+} has substituted both Na^+ and Ca^{2+} in the structure. ICP-MS measurements of the phase digested in nitric acid give a U/Eu ratio of 2.05 indicating that a significant amount of Eu(III) has been taken into solid phase.

Vibrational spectroscopy is very useful in the carbonate family of uranyl minerals, as the U=O and CO_3^{2-} bands are diagnostic of differing coordination environments. The Raman and infrared spectra of synthetic and natural andersonite have been reported previously,[20,39] and our spectra are consistent with these (Table 2); we have also prepared andersonite in D_2O and the deuterated spectra are shown in Fig. S16 and 17;† as might be expected from the structure, where the water mole-

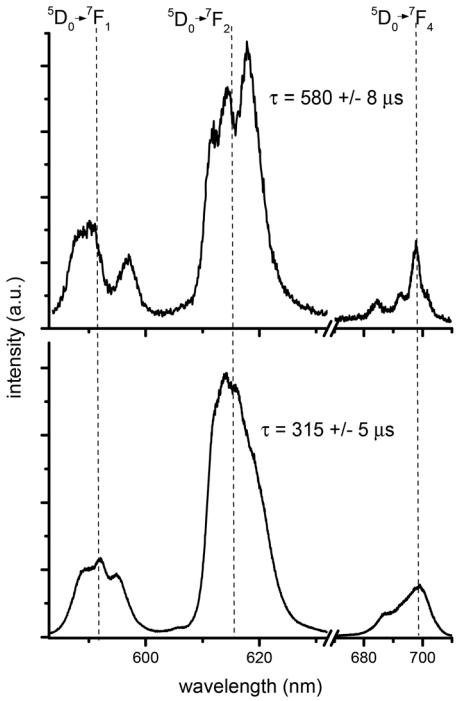

Fig. 3 10 K solid-state emission spectra of Eu^{3+} incorporated andersonite (top, λ_{ex} = 577.88 nm) and grimselite (bottom, λ_{ex} = 579.18 nm).

cules are only coordinated to the Na^+ and Ca^{2+} ions the uranyl and carbonate bands are unaffected in the deuterated spectra. Upon addition of Eu(III), the U═O band in the Raman spectra changes from 816 to 833 cm^{-1} indicating a shortening of the U═O bond length of 0.01 Å using the Bartlet and Cooney formulae (Fig. S16 and 17†). The ν_3(CO) bands in the IR spectrum also change, both in position and in the multiplicity, suggesting an undistorted C_{2v} symmetry around the bridging carbonate ion. This is in contrast to andersonite where they are non-equivalent, as expected from the structural analysis. The infrared spectra of europium carbonates[40] show the ν_3(CO) bands above 1500 cm^{-1} indicating that the carbonate remains bound to uranyl in a bidentate fashion (1372 and 1505 cm^{-1}).

Grimselite shows different behaviour to andersonite as attempted synthesis in the presence of Eu(III) afforded only single crystals of grimselite, with no Eu incorporation or sorption. We have conducted a number of experiments using Th(IV) {as a surrogate for Pu(IV)} and some of the later lanthanides {Tb(III), Er(III) and Yb(III)}, which only afford single crystals of grimselite, as determined by single crystal X-ray diffraction. In contrast, europium emission was observed from grimselite *via* the contacting methodology. Unfortunately addition of europium to single crystals of grimselite in a number of solvents *via* this method affords rapid degradation of the crystal and a resultant powder was formed over the period of 1–2 hours. The emission spectra of these powders were measured at room temperature and, irrespective of the wavelength used for excitation, only Eu(III) emission was observed (Fig. S4†); although the peaks were very broad, a similar emission profile to andersonite was observed. However in this case a weak $^5D_0 \rightarrow {}^7F_0$ transition was observed at λ_{em} = 577.9 nm.

Table 2 Vibrational data for andersonite, grimselite and liebigite and their corresponding Eu(III) complexes including the Eu(III) lifetime data recorded at room temperature

Mineral	ν_1(U═O) cm^{-1}	ν_3(U═O) cm^{-1}	$\nu_3(CO_3)$ cm^{-1}	τ (RT) μs	τ (10 K) μs
Andersonite	806	913	1375	—	—
	832	899	1347		
			1523		
			1558		
			1578		
D-Andersonite	832	886	1374	—	—
Andersonite + Eu	833	895	1372	51, 155	580 ± 8
			1505		
D-Andersonite + Eu	834	905	1376	72, 262	—
			1515		
Grimselite	815	876	1337	—	—
			1538		
D-Grimselite	812	874	1336	—	—
			1541		
Grimselite + Eu	813	901	1372	34, 171	315 ± 5
			1515		
D-Grimselite + Eu	814	896	1372	17, 342	—
			1512		
Liebigite	829	870	1377	—	—
		906	1505		
D-liebigite	831	901	1505	—	—
		871	1386		
Liebigite + Eu	829	870	1380	14, 127	—
		906	1516		
D-Liebigite + Eu	823	871	1404	39	—
		918	1500	244	

The lifetimes of the Eu^{3+} contacted grimselite and the deuterated analogues were used to calculate the hydration number $q = 3.1 \pm 0.5$ (Table 2). The quantum yield ($\Phi = 0.67\%$) is again lower than $EuCl_3$. A low temperature photophysical investigation was next undertaken in order to resolve the broad bands and allow an assignment of the symmetry of the Eu^{3+} ions (Fig. 3). The excitation spectra showed only one Eu^{3+} species (Fig. S10†) but spectral resolution of the emission was not as enhanced as for the other compounds studied. Curve fitting analysis (Fig. S18†) showed a threefold splitting of the $^5D_0 \rightarrow {}^7F_1$ transition and a resolved fourfold splitting of the $^5D_0 \rightarrow {}^7F_2$ transition. This suggests site symmetry of C_{2v}; however in this case the $^7F_2$ transition should be split fivefold which is not resolvable in our case due to the broadness of the bands, possibly because of the crystallinity of the system or the rigidity of the lattice site. The low temperature europium lifetime ($\tau = 315 \pm 5$ μs) is mono-exponential and results in $q = 2.8 \pm 0.5$. SEM (Fig. S19†) images again show a morphology change upon addition of Eu^{3+}, as might be expected from the crystal degradation, and EDX (Fig. S20†) shows no sodium is present – *i.e.* Eu(III) has substituted only Na^+ and not K^+ in the structure, in agreement with the respective difference in ionic radii. The U/Eu ratio is 4.00 according to ICP-MS measurements.

As in the previous examples, the vibrational spectra have been examined. The vibrational data for grimselite has not been previously reported (Table 2 and Fig. S21, 22†) but are in keeping with the structure, *i.e.* one carbonate environment and only one U=O bond stretch; interestingly, compared to andersonite there is a shift to lower frequencies for the U=O stretch that could be due to the CCIs in the structure. When grimselite is synthesized in D_2O only a powder is obtained, but the vibrational spectra are identical. Upon Eu^{3+} incorporation there is a broadening of the Raman active U=O stretch and the carbonate bands shift to higher wavenumbers, as was observed in andersonite (Fig. 4).

Finally, we have examined liebigite to elucidate the influence of its different structure compared to the previous carbonates on the uptake of Eu(III). Addition of Eu(III) affords a powder that is only weakly luminescent under a UV lamp. In keeping with this the quantum yield was too low to be accurately measured. The room temperature emission spectrum is shown in Fig. S23† and again shows sensitized Eu(III) emission. The emission spectra is very broad, but the lifetime ($\tau = 126 \pm 27$ μs) gives a hydration number $q = 7.9 \pm 0.5$. EDX measurements show Ca is still present (Fig. S22†) and ICP-MS measurements gives a U/Eu ratio of 4.00. The presence of sensitized emission suggests that it is not a simple outer-sphere complex formed on the surface. The vibrational data (Table 2 and Fig. S26, 27†), shows little change from that of liebigite[41] and is consistent with the structural data where the Ca^{2+} ions are fully hydrated and not engaged in CCIs.[36] As in the case of becquerelite, the hydrogen bonded network is also disrupted and the O···O bond lengths change from 2.850 Å (3455 cm^{-1}) to 2.776 Å (3361 cm^{-1}), 2.976 Å (3541 cm^{-1}) and 3.075 Å (3568 cm^{-1}). These data suggests that the Eu^{3+} has exchanged some of the calcium ions in the layers of the uranyl carbonate sheets, which has a similar layered structure to becquerelite, and the europium ions are fully hydrated and not involved in any CCIs.

Whilst from our data it is not possible to suggest what charge balancing mechanism is responsible for the substitution of the cations in the carbonate minerals, nevertheless it is an important observation that Eu(III), and therefore by inference Am(III), can be included in the structure. We were also interested in how readily the Eu(III) ions can be removed from the mineral phases as this will have important implications for long term storage of SNF. In order to examine this we have treated the four compounds described above with an aqueous solution of 0.01 M EDTA and monitored the solid phases by ICP-MS, after digestion in nitric acid. Interestingly for the case of becquerelite, andersonite and liebigite the ratio of U : Eu stays effectively constant, whilst for grimselite the europium ions are almost totally removed. However europium incorporated grimselite is stable in water for at least 6 months, without apparent leaching Eu(III) ions (as judged by emission spectroscopy of the aqueous phase). This, in combination with the andersonite results described above, suggest that when the contacting methodology is used a rather weak inner-sphere complex is formed and Eu(III) can be removed, whereas when the co-precipitation method is used the Eu(III) ions form an incorporation complex.

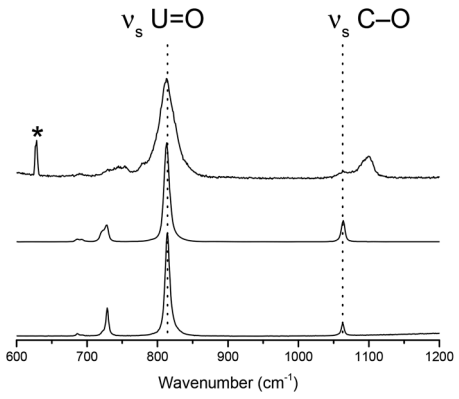

Fig. 4 Raman spectra of deuterated grimselite (bottom), grimselite (middle) and grimselite contacted with $EuCl_3$ (top) (* = artefact in measurement).

Synthesis of a mixed metal uranyl nitrate

During the synthesis of andersonite in the presence of Eu(III), we were able to isolate a small amount of crystalline material that did not have the same diffraction data as andersonite. Refinement of the structure shows an unexpected sodium calcium-uranyl nitrate compound with an empirical formula of $Ca_{56}N_{144}Na_{80}O_{992}U_{96}$, which assembles into a 3D framework; the asymmetric unit is shown in Fig. 5 top and the packing shown in Fig. 5 bottom. It should be noted that the voids contain diffuse atoms that could not be satisfactorily refined and removed using SQUEEZE. In addition no hydro-

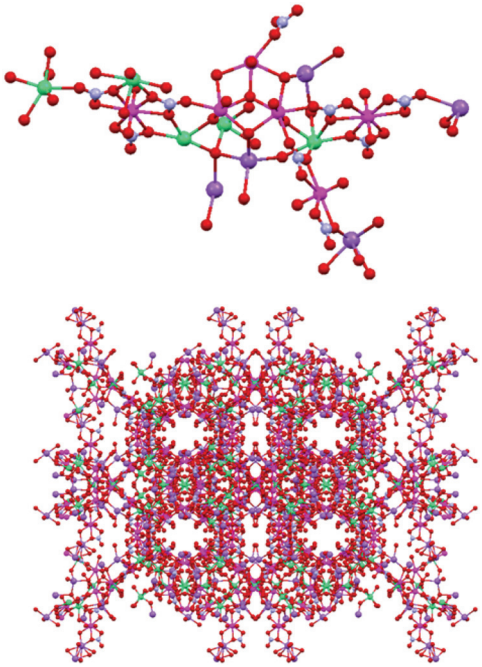

Fig. 5 Asymmetric unit (top) and packing diagram viewed down the *b*-axis (bottom). Color code: U = pink; O = red; Ca = green, Na = purple, N = blue.

gens were located or refined on the water molecules so although the voids look empty they are likely filled with water molecules; the solvent accessible volume = 14 125 Å^3. Upon isolation the crystalline material rapidly degrades to a powder, suggesting that the solvent is important in the stability of the framework. Some precedent exists for mixed metal carbonates that have been isolated from the synthesis of andersonite,[42] or the related $Na[UO_2(NO_3)_3]$[43] which both have extended structures, whilst Uranium Organic Frameworks (UOFs) and hybrid inorganic–organic uranyl frameworks are known.[44] The asymmetric unit consists of uranyl ions coordinated to three nitrate ions which also coordinate to Na^+ or Ca^{2+} ions, and a uranyl trimer linked by a μ_3- and a μ_2-oxo group. The bond lengths for the U–O bonds of the μ_3-O fragment are 2.240(7), 2.253(7) and 2.252(7) Å, typical for this bond.[45] The bond lengths for the μ_2-oxo average 2.394 Å. Two of the uranyl –yl oxygen atoms interact with Cs ions, but the U═O bond lengths are identical and typical for a uranyl ion (1.76–1.81 Å), as are the U–O bonds of the nitrate (2.409(9) to 2.448(7) Å). The IR spectrum of this complex (Fig. S28†) shows a very broad band centred at 1345 cm^{-1} due to the symmetric and asymmetric N–O stretch, a band at 830 cm^{-1} due to the δ(N–O) and the ν_3(U═O) stretch at 900 cm^{-1}. The ν_1(U═O) stretch appears at 834 cm^{-1} in the Raman spectra (Fig. S29†). EDX measurements confirmed the presence of only uranium, calcium and sodium as the metal components.

Americium tracer experiments

The Eu(III) experiments discussed above have shown that for the mineral phases becquerelite, andersonite, grimselite and liebigite we predict that ^{241}Am(III) may interact with these and thus retard migration under environmental conditions. Whilst it was not possible for us to conduct experiments on a macroscopic scale, we have used tracer studies to explore this hypothesis. Thus, reactions of a 200 Bq solution of $^{241}AmCl_3$ in dilute acid with the mineral phases under the conditions of Eu(III) incorporation, specifically a co-precipitation methodology for becquerelite, andersonite and liebigite and a contact methodology for grimselite, we were able to quantify the amount of americium associated with the solid using gamma spectroscopy (a typical spectra is shown in Fig. S30†). We also included compreignacite in our study as this does incorporate Np(V)[6a] even though Eu(III) does not. The results of this investigation are shown in Table 3. The distribution ratio, *D*, can be defined as the ratio of the activity of ^{241}Am in the solid compared to the liquid, and these data are also given in Table 3. From these measurements, and under our experimental conditions, americium(III) is included in the structure but not to a large extent. There does appear to be a qualitative correlation between the amount of Eu^{3+} and Am^{3+} included, when comparing the ratio of the Eu to U concentrations measured from ICP-MS analysis and the Am : U activity (Table 3). Thus becquerelite incorporates the least amount of Eu and Am, whist the carbonate minerals and notably grimselite the most. However the data does not allow us to draw any conclusions as to the chemical environment of the americium or uranium. Therefore we have measured the Raman and emission spectra of these solid compounds. Raman spectroscopy (Table 3 and Fig. S31†) shows small shifts in the ν_1(U═O) bond stretching frequency from the mineral, and are comparable to that

Table 3 Quantification of ^{241}Am from γ-spectrometric, Raman and emission spectroscopic results from ^{241}Am(III) incorporation studies

Mineral	^{241}Am(Bq)/mg of mineral	Bq of ^{241}Am/Bq of $^{238}U^a$	*D*	ν_1(U═O) cm^{-1}	λ_{em} (nm)
Compreignacite	0.91	0.08	Not determined	827 850	686
Andersonite	0.77	0.06 (0.42)	0.0868	828	686
Liebigite	1.83	0.23 (0.17)	2.186	830	688
Grimselite[b]	3.2	0.21 (0.69)	0.2592	810	687
Becquerelite	0.012	0.0026 (0.11)	6.95×10^{-4}	838	[c]

[a] Values in parentheses are the Eu : U ratio from the analogous reactions with Eu, as determined by ICP-MS. [b] *Via* a contact methodology. [c] Below the limit of detection for our spectrometer.

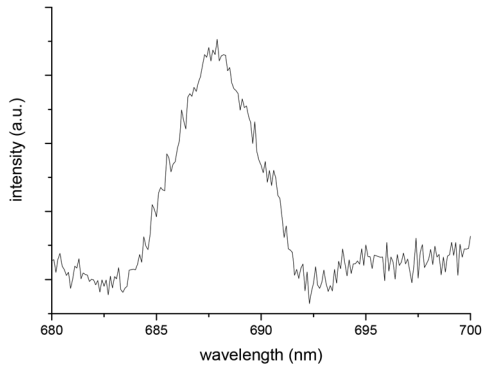

Fig. 6 Solid-state emission spectrum of $^{241}Am^{3+}$ incorporated leibigite at room temperature (λ_{ex} = 504 nm).

observed in the Eu(III) compounds. Fluorescence spectroscopy of Am(III) has been utilised in sorption studies,[46] although the low quantum yield and short lifetimes means that Cm emission is a more favoured ion for such studies.[47] Nevertheless, the $^5D_1 \rightarrow {}^7F_1$ transition at 685 nm is somewhat diagnostic. For instance, in the aqua complex λ_{em} = 685 nm whilst for the carbonate complex $[Am(CO_3)_3]^{3-}$ this maxima shifts to 693 nm.[46c] The solid state emission spectra of liebigite is shown in Fig. 6 whilst for andersonite, grimselite and compreignacite these are shown in Fig. S32;† for becquerelite, the mineral with the lowest amount of americium we observed no emission spectra. In general the spectra are similar, which show a broad peak with the maxima around 687 nm (Table 3). This suggests that the americium ion keeps its hydration shell to an extent, although we were not able to measure the lifetimes to confirm this. Importantly however, there is no evidence for the formation of americium carbonates. Interestingly no uranyl emission is observed, even when excited at bands specific to the uranyl ion. The excitation spectrum of grimselite contacted with $^{241}Am^{3+}$ shows the presence of a band assigned to the –yl MLCT transition (Fig. S33†). The quenching effect of Am(III) on UO_2^{2+} has not been reported previously, but may not be unexpected. Also of note is that the concentrations of the Am in the solids are *ca.* 10^{-6} M so emission spectroscopy could be more useful in speciation studies than is typically used. Therefore, given the similarities in spectroscopic data between the americium and europium incorporated minerals we suggest that americium does incorporate into the minerals *via* ion exchange under the conditions of our experiments.

Conclusions

In conclusion, the reaction of Eu(III) and Am(III) with a series of environmentally relevant uranyl minerals has been reported and summarized in Table 4. A photophysical investigation has revealed that some uranyl minerals can incorporate Eu^{3+} into their structure and this leads to a sensitisation of the europium emission. Low temperature emission spectra show

Table 4 Summary of Eu and Am interactions with selected minerals

Mineral	Eu after contact	Eu after co-precipitation	Am interaction
Schoepite	–	–	Not predicted
Compreignacite	–	–	+
Becquerelite	–	+	+
Andersonite	+	+	+
Grimselite	+	–	+
Liebigite	–	+	+
meta-Autunite	–	–	Not predicted
meta-Torbernite	–	–	Not predicted
Cuprosklodowskite	–	–	Not predicted
Studtite	–	–	–

sufficient spectral enhancements to allow the symmetry of the Eu(III) environments to be deduced. Analysis of the IR and Raman spectra, in combination with ICP-MS, SEM and EDX techniques, gives further support to the conclusions. Thus, for becquerelite and liebigite calcium is exchanged in the interlayer but for the carbonates grimselite and andersonite the europium is incorporated into the structure with low hydration numbers. The observation of sensitised emission suggests that the uranyl and europium ions are in close proximity to each other and vibrational data is consistent with presence of cation–cation interactions in some of these. Importantly our results suggest Am(III) could be incorporated into minerals and experiments at a tracer level prove this, although the amount of Am(III) incorporation is quite low. From a point of view of repository safety, our results suggest that these oxidative phase changes on the surface of SNF could possibly mitigate, but not completely retard the migration of americium into the near field environment.

Experimental

Caution! Although depleted uranium was used during the course of the experimental work, as well as the radiological hazards uranium is a toxic metal and care should be taken with all manipulations. ^{241}Am is an α and γ emitter, and all experiments were carried out in a laboratory designated for the use of radioactive isotopes. Experiments using radioactive materials were carried out using pre-set radiological safety precautions in accordance with the local rules of Trinity College Dublin and HZDR.

IR spectra were recorded on a Perkin Elmer Spectrum One spectrometer with attenuated total reflectance (ATR) accessory. Raman spectra were obtained using 785 nm excitation on a Renishaw 1000 micro-Raman system. Room Temperature steady-state photoluminescence spectra were recorded on a Horiba-Jobin-Yvon Fluorolog-3 or Fluoromax spectrofluorimeter. Luminescence lifetime data were recorded following 375 nm excitation, using time-correlated single-photon counting (a PCS900 plug-in PC card for fast photon counting). Lifetimes were obtained by tail fit on the data obtained, and the quality of fit was judged by minimization of reduced

chi-squared and residuals squared. Quantum yield measurements were recorded using a Horiba-Jobin-Yvon F-3018 PLQY integrating sphere. For the ^{241}Am experiments the spectra were fitted to a Gaussian curve function using Origin software. Low temperature time resolved luminescence measurements were excited using a tuneable Radiant Dyes NarrowScanK dye laser, collected by an optical fiber and transmitted into a spectrograph (Acton Research, USA). The resolved spectrum is measured by an intensified charge-coupled device camera system (Roper Scientific, USA). SEM microscopy were conducted on a Tescan MIRA XMU Scanning Electron Microscope (SEM) with a backscatter detector and imaged at 20 kV. The EDX (energy dispersive X-ray analyzer) measurements were recorded on an Oxford INCA XMAX. The samples were mounted on carbon tabs and coated in carbon. ICP-MS was collected on a Thermo (Thermo Fischer Scientific) iCapQc ICP-QMS, using an ESI (Elemental Scientific, Inc.) brand SC-2DX microFAST 1 sample introduction system fitted with a 1 ml loop; USGS standard W-2 was used as the calibration standard. A known amount of sample was digested in triply distilled 2% HNO_3 and 8 runs were collected per sample and the average taken. Singe crystal X-ray diffraction data were measured on a Bruker Apex diffractometer. Further details of the crystal structure investigation can be obtained from the Fachinformationszentrum Karlsruhe, 76344 Eggenstein-Leopoldshafen, Germany (fax: (+49)7247-808-666; e-mail: crysdata@fiz-karlsruhe.de) on quoting the depository number CSD 429820. The uranyl compounds schoepite,[48] compreignacite,[49] becquerelite,[49] andersonite,[20] grimselite[38] and *meta*-torbernite[8a] were prepared *via* literature methods, whilst *meta*-autunite, hydrated lanthanide chlorides and carrier-free $^{241}AmCl_3$ (Perlamar) were obtained commercially. The Am-241 measurements were carried out by high-resolution gamma spectrometry using an n-type high-purity germanium detector (EG&G Ortec model GMX-15190) with a relative efficiency of 19% and a resolution of 1.90 keV (FWHM) at 1.33 MeV; this gives a total error of 15% in the measurements. The activities calculated as described in ref. 50.

Contact procedure. To a suspension of crystalline grimselite (0.30 g) in milipure water (5 cm^3) was added 1 cm^3 of a 1 M solution of $EuCl_3$ in water and the mixture stirred for 24 hours. The resulting powder was isolated by filtration and washed with water (3 × 20 cm^3) then air dried.

Synthesis of Eu + andersonite. To a solution of uranyl nitrate (1.0 cm^3 of a 2.0 M solution), calcium nitrate (1.0 cm^3 of a 2.0 M solution) and sodium carbonate (3.0 cm^3 of a 2.0 M solution) in 10 ml of water was added 1.0 ml of a 2.0 M solution of $EuCl_3$ in water and the mixture was stirred overnight, then stood for 7 days to afford a yellow precipitate. After filtration the solid was washed with copious water then dried in vacuum desiccator containing anhydrous $CaCl_2$. The mother liquor was kept in an open flask and after approx. two weeks a small amount of crystalline material (<10 mg) formed, which was isolated and characterized by X-ray diffraction and vibrational spectroscopy.

Synthesis of Eu + leibigite. To a solution of uranyl nitrate (1.0 cm^3 of a 2.0 M solution), calcium nitrate (1.0 cm^3 of a 2.0 M solution) and sodium carbonate (3.0 cm^3 of a 2.0 M solution) in 10 ml of water was added 1.0 ml of a 2.0 M solution of $EuCl_3$ in water and the mixture was stirred overnight, then stood for 7 days to afford a yellow precipitate. After filtration the solid was washed with copious water then dried in vacuum desiccator containing anhydrous $CaCl_2$.

Synthesis of Eu + becquerelite. A solution of uranyl acetate (1.0 cm^3 of a 2.0 M solution), calcium nitrate (1.0 cm^3 of a 0.16 M solution) and $EuCl_3$ (1.0 ml of a 2.0 M solution) was heated to 140 °C in a sealed Schleck containing a J. Young attachment for 3 days.

Treatment of Eu phases with EDTA. To a suspension of 50 mg of the Eu containing phase in water (10 cm^3) was added a solution of EDTA (0.01 M in water). This was stirred for 12 hours and the solid isolated by filtration and dried. This was then dissolved in triply distilled 2% HNO_3 and analysed by ICP-MS.

Typical ^{241}Am reaction procedure. To a solution of uranyl nitrate (1.0 cm^3 of a 2.0 M solution), calcium nitrate (1.0 cm^3 of a 2.0 M solution) and sodium carbonate (3.0 cm^3 of a 2.0 M solution) in 10 ml of water was added 1.0 ml of a 200 Bq solution of $^{241}AmCl_3$ in 0.1 M HCl and the mixture was stood for 7 days to afford a yellow precipitate. The supernatant was carefully removed using a pipette and the solid washed with water and air dried.

Acknowledgements

We thank Irish Research Council for funding this work *via* a Government of Ireland Postdoctoral Fellowship (SB), Prof. Balz S. Kamber from the Department of Geology at TCD for assistance with ICP-MS measurements and the Centre for Microscopy and Analysis at TCD for the SEM and EDX measurements. This work was co-financed (M. S.) by the Helmholtz Gemeinschaft Deutscher Forschungszentren (VH-NG-942) and (R. S.) from the Federal Ministry of Education and Research (BMBF) under grant 02NUK019D.

Notes and references

1 W. E. Falck and K.-F. Nilsson, Geological disposal of radioactive waste: moving towards implementation, *Joint Research Centre Reference Report*, EUR23925, 2009.
2 L. H. Johnson and D. W. Shoesmith, in *Radioactive Waste Forms for the Future*, ed. W. Lutze and R. C. Ewing, Elsevier, 1988, 635.
3 A. Mesbah, S. Szenknect, N. Clavier, J. Lozano-Rodriguez, C. Poinssot, C. Den Auwer, R. C. Ewing and N. Dacheux, *Inorg. Chem.*, 2015, **54**, 6687.
4 R. J. Baker, *Coord. Chem. Rev.*, 2014, **266–267**, 123.

5 J. P. Kaszuba and W. H. Runde, *Environ. Sci. Technol.*, 1999, **33**, 4427.
6 (*a*) P. C. Burns, K. M. Deely and S. Skanthakumar, *Radiochim. Acta*, 2004, **92**, 151; (*b*) A. L. Klingensmith, K. M. Deely, W. S. Kinman, V. Kelly and P. C. Burns, *Am. Mineral.*, 2007, **92**, 662; (*c*) M. Douglas, S. B. Clark, J. I. Friese, B. W. Arey, E. C. Buck, B. D. Hanson, S. Utsunomiya and R. C. Ewing, *Radiochim. Acta*, 2005, **93**, 265.
7 (*a*) A. L. Klingensmith and P. C. Burns, *Am. Mineral.*, 2007, **92**, 1946; (*b*) D. S. Alessi, J. E. S. Szymanowski, T. Z. Forbes, A. N. Quicksall, G. E. Sigmon, P. C. Burns and J. B. Fein, *J. Nucl. Mater.*, 2013, **433**, 233.
8 (*a*) N. A. Meredith, M. J. Polinski, J. N. Cross, E. M. Villa, A. Simonetti and T. E. Albrecht-Schmitt, *Cryst. Growth Des.*, 2013, **13**, 386; (*b*) L. C. Shuller, R. C. Ewing and U. Becker, *J. Nucl. Mater.*, 2013, **434**, 440; (*c*) L. C. Shuller, R. C. Ewing and U. Becker, *Am. Mineral.*, 2010, **95**, 1151.
9 P. C. Burns, R. C. Ewing and M. L. Miller, *J. Nucl. Mater.*, 1997, **245**, 1.
10 S. E. Binney, C. H. Bloomster, H. R. Brager, C. A. Burgess, W. J. Gruber, G. F. Howden, A. J. Naser, L. G. Niccoli, A. W. Prichard, J. A. Rawlins, G. W. Reddick, W. W. Schulz, J. P. Sloughter, J. L. Swanson, J. W. Thorton, C. N. Wilson and D. E. Wood, Clean Use of Reactor Energy, *Report WHC-EP-0268*, Westinghouse Hanford Company, Richland, WA, 1990.
11 W. Runde, in *Radionuclides in the Environment*, ed. D. A. Atwood, John Wiley & Sons, Ltd, Weinheim, 2010, vol. 2, 315.
12 For a recent review see: H. Geckeis, J. Lützenkirchen, R. Polly, T. Rabung and M. Schmidt, *Chem. Rev.*, 2013, **113**, 1016.
13 C. Mallon, A. Walshe, R. J. Forster, T. E. Keyes and R. J. Baker, *Inorg. Chem.*, 2012, **51**, 8509.
14 B. McNamara, B. Hanson, E. Buck and C. Soderquist, *Radiochim. Acta*, 2005, **83**, 169.
15 R. D. Shannon, *Acta Crystallogr., Sect. A: Cryst. Phys., Diffr., Theor. Gen. Cryst.*, 1976, **32**, 751.
16 K. Binnemans, *Coord. Chem. Rev.*, 2015, **295**, 1.
17 J. Kuta, Z. Wang, K. Wisuri, M. C. F. Wander, N. A. Wall and A. E. Clark, *Geochim. Cosmochim. Acta*, 2013, **103**, 184.
18 Y. Wang, X. Yin, Y. Zhao, Y. Gao, L. Chen, Z. Liu, D. Sheng, J. Diwu, Z. Chai, T. E. Albrecht-Schmitt and S. Wang, *Inorg. Chem.*, 2015, **54**, 8449.
19 C.-W. Kim, D. J. Wronkiewicz, R. J. Finch and E. C. Buck, *J. Nucl. Mater.*, 2006, **353**, 147.
20 S. Amayri, T. Arnold, T. Reich, H. Förstendorf, G. Geipel, G. Bernhard and A. Massanek, *Environ. Sci. Technol.*, 2004, **38**, 6032.
21 S. Amayri, T. Arnold, H. Förstendorf, G. Geipel and G. Bernhard, *Can. Mineral.*, 2004, **42**, 953.
22 S. Amayri, T. Reich, T. Arnold, G. Geipel and G. Bernhard, *J. Solid State Chem.*, 2005, **178**, 567.
23 See for example: (*a*) S.-P. Liu, M.-L. Chen, B.-C. Chang and K.-H. Lii, *Inorg. Chem.*, 2013, **52**, 3990; (*b*) G. H. Jia and P. A. Tanner, *J. Alloys Compd.*, 2009, **471**, 557; (*c*) S. Maja and K. S. Viswanathan, *J. Lumin.*, 2009, **129**, 1242; (*d*) E. A. Seregina, A. A. Seregin and G. V. Tikhonov, *J. Alloys Compd.*, 2002, **341**, 283; (*e*) S. Dai, W. Xu, D. H. Metcalf and L. M. Toth, *Chem. Phys. Lett.*, 1996, **262**, 315; (*f*) T. Yamamura, Z. Fazekas, M. Harada and H. Tomiyasu, *Phys. Chem. Chem. Phys.*, 1999, **1**, 3491; (*g*) M. Lopez and D. J. S. Birch, *J. Lumin.*, 1987, **71**, 221; (*h*) Y. Okamoto, Y. Ueba, I. Nagata and E. Banks, *Macromolecules*, 1981, **14**, 807; (*i*) S. P. Tanner and A. R. Vargenas, *Inorg. Chem.*, 1981, **20**, 4384; (*j*) R. Reisfeld, N. Lieblich, L. Boehm and B. Barnett, *J. Lumin.*, 1976, **12**, 749; (*k*) J. L. Kropp, *J. Chem. Phys.*, 1967, **46**, 843.
24 W. D. Horrocks and D. R. Sudnick, *J. Am. Chem. Soc.*, 1979, **101**, 334.
25 This approach has been reported previously for $Nd[(UO_2)_3O(OH)(PO_4)_2]\cdot 6H_2O$: C. A. Armstrong, K. L. Nash, P. R. Griffiths and S. B. Clark, *Am. Mineral.*, 2011, **96**, 417.
26 (*a*) C. Edder, C. Piguet, J.-C. G. Bünzli and G. Hopfgartner, *Chem. – Eur. J.*, 2001, **7**, 3014; (*b*) W. D. Horrocks and D. R. Sudnick, *Acc. Chem. Res.*, 1981, **14**, 384; (*c*) W. D. Horrocks, B. Holmquist and B. L. Vallee, *Proc. Natl. Acad. Sci. U. S. A.*, 1975, **72**, 4764.
27 M. Schmidt, S. Heck, D. Bosbach, S. Ganschow, C. Waltherd and T. Stumpf, *Dalton Trans.*, 2013, **42**, 8387.
28 (*a*) M. Schmidt, T. Stumpf, M. Marques Fernandes, C. Walther and T. Fanghänel, *Angew. Chem., Int. Ed.*, 2008, **47**, 5846; (*b*) M. Marques Fernandes, M. Schmidt, T. Stumpf, C. Walther, D. Bosbach, R. Klenze and Th. Fanghänel, *J. Colloid Interface Sci.*, 2008, **321**, 323; (*c*) L. Z. Lakshtanov and S. L. S. Stipp, *Geochim. Cosmochim. Acta*, 2004, **68**, 819.
29 P. A. Tanner, *Chem. Soc. Rev.*, 2013, **42**, 5090.
30 T. Kimura and G. R. Choppin, *J. Alloys Compd.*, 1994, **213–214**, 313.
31 J. R. Bartlett and R. P. Cooney, *J. Mol. Struct.*, 1989, **193**, 295.
32 R. J. Baker, *Chem. – Eur. J.*, 2012, **18**, 16258.
33 P. C. Burns and Y. Li, *Am. Mineral.*, 2002, **87**, 550.
34 E. Libowitzky, *Monatsh. Chem.*, 1999, **130**, 1047.
35 R. L. Frost, J. Cejka and M. L. Weier, *J. Raman Spectrosc.*, 2007, **38**, 460.
36 K. Mereiter, *Tscher. Miner. Petrog.*, 1982, **30**, 277.
37 A. Coda, A. Della Giusta and V. Tazzoli, *Acta Crystallogr., Sect. B: Struct. Crystallogr. Cryst. Chem.*, 1981, **37**, 1496.
38 Y. Li and P. C. Burns, *Can. Mineral.*, 2001, **39**, 1147.
39 R. L. Frost, O. Carmody, K. L. Erickson, M. L. Weier and J. Čejka, *J. Mol. Struct.*, 2004, **703**, 47.
40 W. Runde, C. Van Pelt and P. G. Allen, *J. Alloys Compd.*, 2000, **303–304**, 182.
41 R. L. Frost, K. L. Erickson, M. L. Weier, O. Carmody and J. Čejka, *J. Mol. Struct.*, 2005, **737**, 173.
42 R. Vochten, L. Van Haverbeke, K. Van Springel, N. Blaton and O. M. Peeters, *Can. Mineral.*, 1994, **32**, 553.
43 T. Bäcker and A.-V. Mudring, *Z. Anorg. Allg. Chem.*, 2010, **636**, 1002.

44 For recent examples of uranyl–organic frameworks, see: (*a*) C. L. Cahill and L. A. Borkowski, in *Structural Chemistry of Inorganic Actinide Compounds*, ed. S. V. Krivovichev, P. C. Burns and I. G. Tananaev, Elsevier, Amsterdam, 2007, ch. 11; (*b*) K. X. Wang and J. S. Chen, *Acc. Chem. Res.*, 2011, **44**, 531; (*c*) M. B. Andrews and C. L. Cahill, *Chem. Rev.*, 2013, **113**, 1121; (*d*) F. Abraham, B. Arab-Chapele, M. Rivenet, C. Tamain and S. Grandjean, *Coord. Chem. Rev.*, 2014, **266–267**, 28; (*e*) T. Loiseau, I. Mihalcea, N. Henry and C. Volkringer, *Coord. Chem. Rev.*, 2014, **266–267**, 69.

45 See for example: (*a*) M. Basile, D. K. Unruh, K. Gojdas, E. Flores, L. Streicher and T. Z. Forbes, *Chem. Commun.*, 2015, **51**, 5306; (*b*) P. Thuéry, *Eur. J. Inorg. Chem.*, 2014, 58.

46 (*a*) T. Stumpf, M. Marques Fernandes, C. Walther, K. Dardenne and Th. Fanghänel, *J. Colloid Interface Sci.*, 2006, **302**, 240; (*b*) Th. Stumpf, C. Hennig, A. Bauer, M. A. Denecke and Th. Fanghaenel, *Radiochim. Acta*, 2004, **92**, 133; (*c*) W. Runde, C. Van Pelt and P. G. Allen, *J. Alloys Compd.*, 2000, **303/304**, 182.

47 L. S. Natrajan, *Coord. Chem. Rev.*, 2012, **256**, 1583.

48 O. Nipruk, A. Knyazev, G. Chernorukov and Y. Pykhova, *Radiochem.*, 2011, **53**, 146.

49 D. Gorman-Lewis, J. B. Fein, P. C. Burns, J. E. S. Szymanowski and J. Converse, *J. Chem. Thermodyn.*, 2008, **40**, 980.

50 G. Gilmore and J. Hemingway, *Practical Gamma Spectrometry*, John Wiley & Sons, Chichester, 1995.